Structural Engineering and Mechanics, *Vol. 53, No. 1 (2015) 1-16*
DOI: http://dx.doi.org/10.12989/sem.2015.53.1.001

Earthquake performance of FRP retrofitting of short columns around band-type windows

Ali Koçak*

Department of Civil Engineering, Yıldız Technical University, 34210, İstanbul, Turkey

(Received January 6, 2014, Revised April 2, 2014, Accepted April 4, 2014)

Abstract. Due to design codes and regulations and the variety of building plans in Turkey, it is very often seen that band-type windows are left for ventilation and lightening of the basements of buildings which are used for various purposes such as workplaces and storage. Therefore when the necessary support measures cannot be given, short columns are subjected to very high shear forces and so damage occurs. One of the precautions to avoid the damage of short column mechanisms in buildings where band-type windows are in the basement is to strengthen the short columns with fiber reinforced polymer (FRP).

In this study, the effect of the FRP retrofitting process of the short columns around band-windowed structures, which are found especially in basement areas, is analyzed in accordance with Turkish Seismic Code 2007 (TSC 2007). Three different models which are bare frame, frame with short columns and retrofitted short columns with FRP, are created and analyzed according to TSC 2007 performance analysis methods to understand the effects of band windows in basements and the effect of FRP retrofitting.

Keywords: performance analysis; short column; reinforced concrete frame; irregular structures; FRP

1. Introduction

It is known that construction and/or design errors have caused a lot of structural damage in buildings during the earthquakes which frequently occur in Turkey. In order to minimize this damage, it is necessary to comply with the rules defined in the legislation for the construction of new buildings. Additionally, existing buildings must be retrofitted/rehabilitated to be resistant to earthquakes or they must be demolished and re-built. Spaces in walls, just like band windows, cause columns which are designed as long columns, to behave as short columns (Fig. 1). These columns exhibit short column behavior under earthquake shaking; they cannot meet the shear forces and have brittle weaknesses (Paulay 1991, Guevara and Garcia 2005, Koçak 2013).

For window openings with heights of 50-60 cm and widths of one column to another, short column behavior can be hindered by adding bricks on both sides of the column or by filling one axis of the windows with bricks. Cracks and breaking owing to shearing forces can be deterred by surrounding the short columns with FRP.

Due to easy application and cost savings for retrofitting purposes, FRP retrofitting is a very common application for column rehabilitation. FRP retrofitting is used very often in reinforced

*Corresponding author, Associate Professor, E-mail: akocak@yildiz.edu.tr

http://www.techno-press.org/?journal=sem&subpage=8 ISSN: 1225-4568 (Print), 1598-6217 (Online)

Fig. 1 Columns showing short column behavior and damage due to band windows

concrete columns and beams, but also for retrofitting in masonry columns, bridges, column-beam joints and short columns. Moreover, it can be said that quite successful results are achieved with this method. In previous studies, there have been many analyses in relation to the effect of FRP retrofitting to structural behavior (Chen 2002). In the study of Toutanji *et al*. (2006), it was demonstrated that the bearing capacities of beams increase significantly in proportion to the increase in the thickness of the FRP, and the ductility decreases. Haskett *et al*. (2009) observed that there is an increase in the torsional capacity and ductility of FRP retrofitted beams. In the study of Wang and Hsua (2008), columns were tested, with a total of 6 different sequences, under axial pressure force until they suffered damage. It could be seen that the bearing forces of FRP retrofitted columns increased. In the case study of Ilki *et al*. (2008), FRP thickness, column section type, stirrup amount, edge angles, loading type (and the application of FRP evaluations whether or not there was any damage) were considered as the main parameters of the study. It was concluded that FRP retrofitted reinforced concrete columns exhibited increased ductility and bearing capacity. In another study of Ilki *et al*. (2009), reinforced concrete columns with low strength concrete and those where the fittings were not used in adequate amounts before and after retrofitting with FRP, were tested with real-sized samples of acting continuous loads and reverse cycle load effects. It was reported that the deformation capacity increased especially in the damaged columns retrofitted with FRP. Hadi (2006) reported that the load bearing capacity and ductility of FRP retrofitted reinforced concrete short columns under axial or eccentric load impact is better than the capacity of non- retrofitted columns. In the study of Kusumawardaningsiha and Hadi (2010), the status of square and round cross sectional columns was analyzed for comparison with the status of short, normal, circular porous and rectangle porous columns and it was found that the FRP retrofitted short columns exhibited an increase in axial load capacity and ductility. Retrofitting short columns with FRP increased the structural displacement and durability capacities of the columns, and test studies demonstrated that these columns exhibited better performance under shear forces (Colomb *et al*. 2008, Yoshimura *et al*. 2000, Promis *et al*. 2009, Chaallal *et al*. 2003, Xiao 2004). In the experimental study by Galal *et al*. (2005), rigid concrete blocks were used and short columns with a rectangular center section, where the ends are constrained, were subjected to cyclic loading from the upper end, and lateral loading was applied to the middle section of the columns. The experiments showed that the shearing forces of FRP retrofitted short columns increased and there was a reduction in the stress of the stirrups. The effects of FRP on the durability of FRP retrofitted short columns and its effects on performance and deformation capacities are also examined. In this study, the effects of the FRP retrofitting to

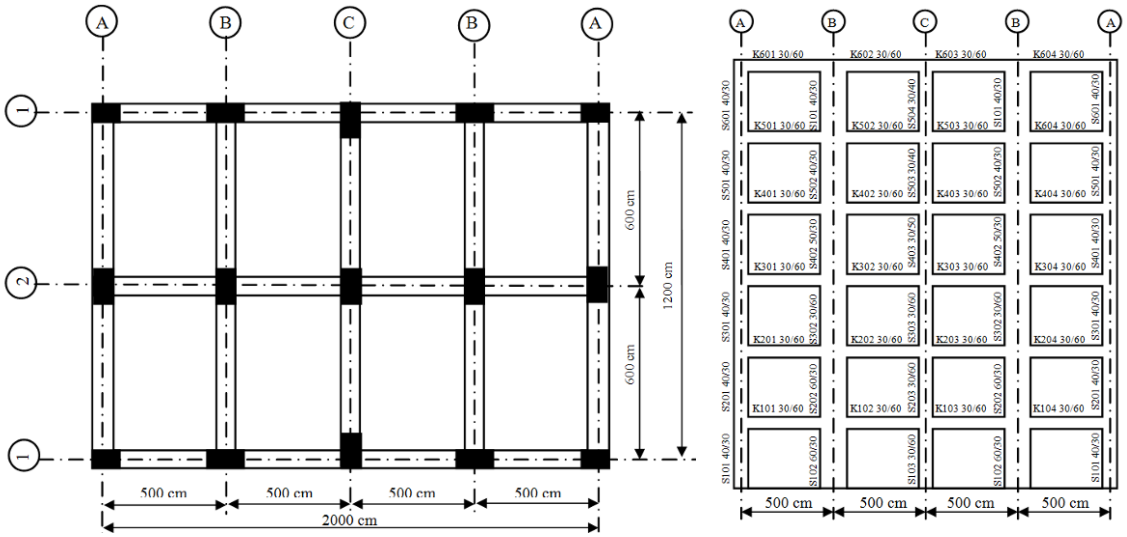

(a) Structure plan (b) Cross section

Fig. 2 Structure plan(a) and cross section(b)

building with the short columns were investigated on a building which has short columns. Three different models which are bare frame, frame with short columns and retrofitted short columns with FRP were modeled and analyzed according to the performance methods of Turkish Seismic Code 2007 (TSC 2007).

2. Numerical analysis

In this study, the status of short columns, which have been made by adding an infill/curtain wall between the frames, in the basement of a building, the plan and cross-section of which are given below (see Fig. 2). For this purpose, a model of a bare frame with continuous openings was used (Girgin 1996). The parameters assumed in the design project of the building and the material parameters are given below.

Assumptions in the design of the building are as follows: 6-storey RC building with 3.5 m storey height was considered within the scope of this study. Considered earthquake zone is 1st degree, the effective ground acceleration coefficient is (A_0) 0.4, the building importance coefficient (I) is 1, the site class is Z2, the spectrum characteristic periods are T_A=0.15s and T_B=0.40s and the load participation factor (n) is 0.3.

The dimensions of the columns are 40/30 cm, 60/30 cm, 30/60 cm, 50/30 cm and 30/50 cm; the dimensions of the beams are 30/60 cm. Compressive concrete strength of the building is 20 MPa and elasticity modulus of the concrete is 28 GPa. The reinforcement steel classifications are S420 and S220 and the elasticity modulus is 200 GPa. The material characteristics of the building and the reinforced concrete details are taken as being in compliance with the project details and accordingly, the building information level was defined as “comprehensive” and the information level coefficient was considered as 1.0.

In the building, which will be subject to pushover analysis, the effective bending rigidity is

Table 1 Effective bending rigidity coefficients of cracked sections in the columns of the 1st floor

Section name	Section type	Width (mm)	Length (mm)	$N_D/(A_c f_{cm})$	Rigidity coefficient
S101	40×30	400	300	0.266	0.621
S102	60×30	600	300	0.291	0.654
S103	30×60	300	600	0.291	0.655
S104	60×30	600	300	0.291	0.654
S105	40×30	400	300	0.266	0.621

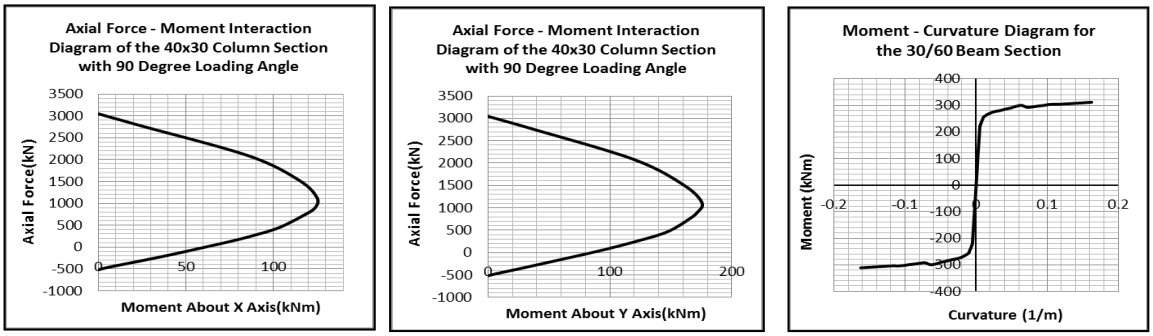

(a) (b) (c)

Fig. 3 Axial force - moment interaction diagrams for the S101 column (a, b), and moment curvature diagram for the 30/60 cm beam (c)

Table 2 Shear force capacity of the columns on the 1st floor

Section name	Section type	Width (mm)	Length (mm)	A_{sw} (mm^2)	V_w (kN)	V_{cr} (kN)	V (kN)
S101	40×30	400	300	100.53	41.47	92.03	115.09
S102	60×30	600	300	100.53	63.59	373.39	362.30
S103	30×60	300	600	100.53	30.41	100.46	110.78
S104	60×30	600	300	100.53	63.59	373.39	362.30
S105	40×30	400	300	100.53	41.47	92.03	115.09

taken as the cracked section of the reinforced concrete being subject to the bending load. The effective bending rigidity belonging to the cracked section is calculated according to the information given in the TSC 2007, which is 0.4 times the bending rigidity of the cracked sections of the beam and columns, based on the value of $N_D/(A_c \times f_{cm})$. The bending rigidity of the cracked sections is given as between 0.4 and 0.8 times. The effective bending rigidity belonging to the cracked sections of the columns in the 1st floor are given in Table 1. The N_D values are axial load values acting on the columns with the load combination $W=G+0.3Q$ where A_c is the section area and f_{cm} is compressive strength of the concrete.

Non-linear behavior is taken into consideration by identifying plastic hinges at the ends of the beams and columns in the analysis of the model. For the plastic hinges, the lumped plasticity model is adopted. Parameters of the plastic hinges are determined by using XTRACT structural cross-section analysis program (Xtract 2001). As an example, the axial force-moment interaction diagrams used for the S101 column (3a, 3b) and moment-curvature diagrams for the beams with a dimension of 30/60 cm (3c) are given in Fig. 3.

Shear-hinges are assigned to the midheight point of the columns of the structure in order to determine the shear failures in the columns. The shear force capacity of the hinges and the columns are given in Table 2.

2.1 Plain frame analysis

Push-over analysis method is used to understand the behavior of the structure during an earthquake. The purpose of this method is to load the building laterally under monotonic loading which is increased step by step until the structural system fails. Period and modal mass participation ratios obtained from modal analysis calculations are given in Table 3.

Load pattern is defined based on first vibration mode shape. The loading values are given in Table 4.

The pushover curve with base shear force versus top displacement is obtained as a result of the loading, and the transformed form of this curve to a modal acceleration - modal displacement diagram, according to TSC' 2007, is given in Figs. 4(a) and 4(b).

Inelastic displacement demand is determined according to TSC 2007 for design spectrum. Fig. 5 shows the static pushover curve and the modal capacity spectrum. Displacement demand of the building is found from Fig. 5(a) as S_{de1}=0.153 m. Accordingly, the top displacement demand is found as given below.

$$S_{d1} = CR_1 \times S_{de1} = 1 \times 0.153 = 0.153\ m \tag{1}$$

$$u_{N1} = \Phi_{N1} \times \Gamma_{x1} \times d_1 = 0.0712 \times 18.936 \times 0.153 = 0.206\ m \tag{2}$$

Table 3 Plain frame systems' periods and modal mass participation ratios for each vibration modes

Mod Number	Period (second)	Vibration direction *Ux* mass participation ratio	Total mass
1	1.230242	0.79641	0.79641
2	0.442564	0.11514	0.91155
3	0.261644	0.04479	0.95634
4	0.193579	0.01491	0.97125
5	0.153954	0.01384	0.98509
6	0.115349	0.01491	1

Table 4 Earthquake load distribution of the direct framed system

Floor number	Cumulative Floor weight (kN)	Floor weight (kN)	1st mode type amplitude (m)	Normalized equal earthquake load distribution
1st Floor	793.06	793.06	0.01010000	0.233
2nd Floor	1589.75	796.69	0.02440000	0.567
3rd Floor	2379.56	789.81	0.03990000	0.918
4th Floor	3161.64	782.08	0.05350000	1.219
5th Floor	3932.96	771.32	0.06550000	1.472
6th Floor	4414.86	481.9	0.07120000	1.000

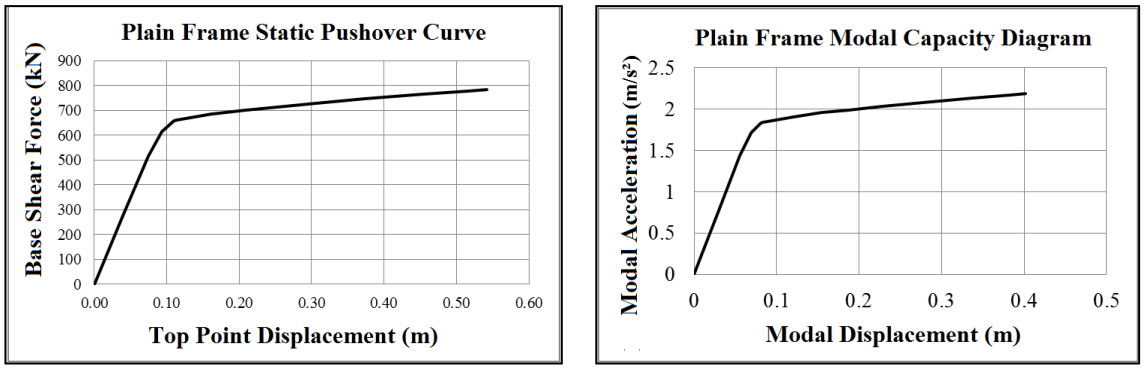

(a) (b)

Fig. 4 (a) Plain-framed system static pushover curve (b) Plain-framed system modal capacity diagram

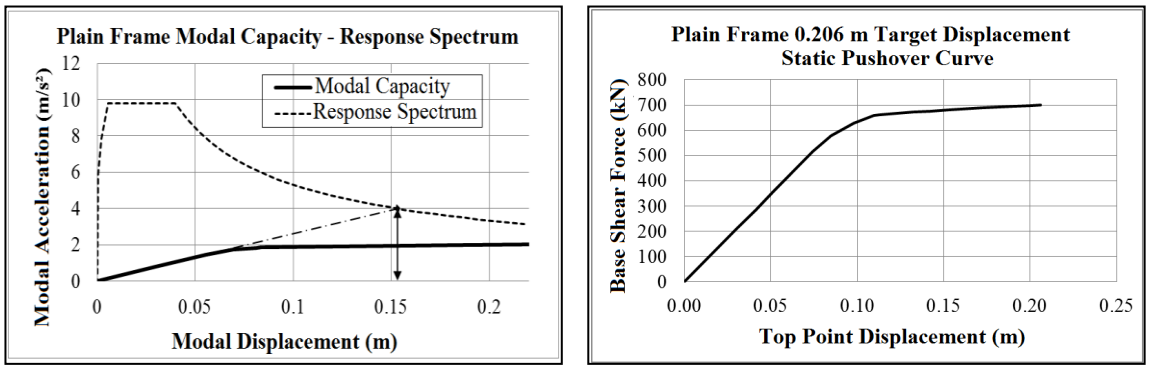

(a) (b)

Fig. 5 (a) Plain-framed system modal capacity and superposed behavior (b) Plain-framed system target displacement pushover curve

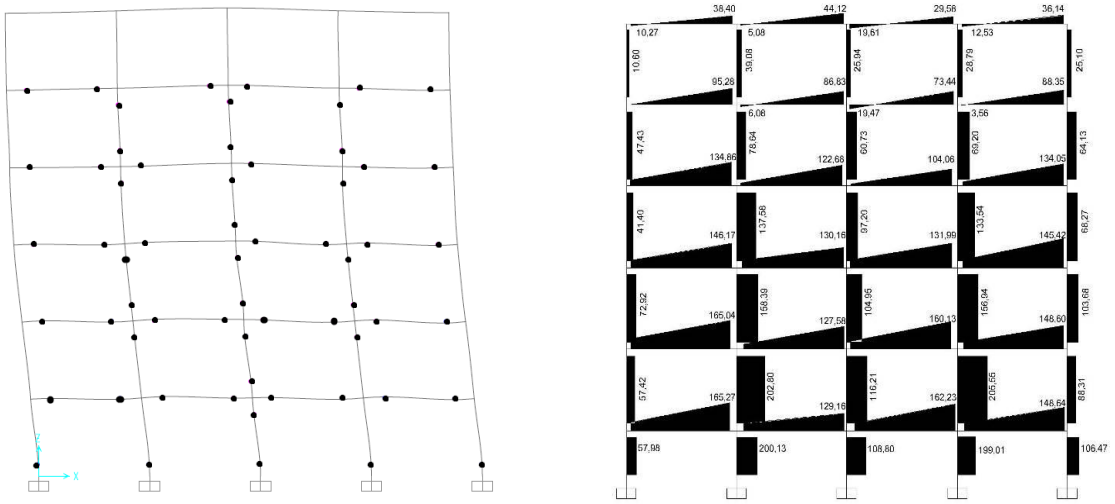

(a) (b)

Fig. 6 (a) Plastic hinges in the last step of the plain frame (b) Shear forces in the last step of the plain frame

The plastic hinges and shear forces occurred in the last step of the static pushover analysis are given in Fig. 6 (a), (b).

2.2 Band-Windowed frame analysis

In order to examine the effect of band windows, an infill wall is added at the bottom of the frame system in order to achieve short columns. Furthermore, shear hinges are assigned to all of the short columns. Period and mass participation ratios achieved from the modal analysis of the band window frame system are given in Table 5. A load distribution that is compatible with first mode modal amplitudes and floor weights is defined as in TSC 2007. The load distribution is shown in Table 6.

The pushover curve and the modal capacity diagram which is transformed form of the pushover curve, are given in Fig. 7.

Table 5 Band window frame system period and mass participation ratios

Mode number	Period (second)	Vibration direction Mass participation ratio	Total mass
1	1.10094	0.69312	0.69312
2	0.393926	0.09985	0.79297
3	0.231948	0.03693	0.8299
4	0.179053	0.01782	0.84772
5	0.136902	0.01719	0.86491
6	0.082682	0	0.86491

Table 6 Band window frame system earthquake load distribution

Floor number	Cumulative Floor weight (kN)	Floor weight (kN)	1st mode type amplitude (m)	Equal earthquake load distribution
1st Floor	793.06	793.06	0.00160000	0.035
2nd Floor	1589.75	796.69	0.01640000	0.357
3rd Floor	2379.56	789.81	0.03550000	0.766
4th Floor	3161.64	782.08	0.05280000	1.127
5th Floor	3932.96	771.32	0.06860000	1.445
6th Floor	4414.86	481.9	0.07600000	1.000

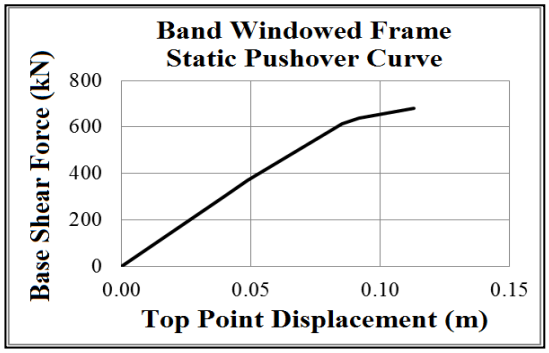

(a)

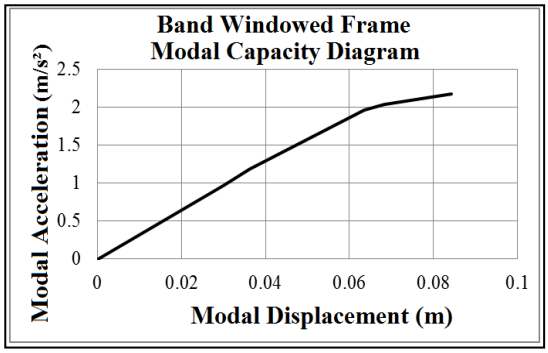

(b)

Fig. 7 (a) Band-windowed frame static pushover curve (b) Band-windowed frame modal capacity diagram

The obtained modal capacity diagram superposed with the design response spectrum and displacement demand is determined according to TSC 2007. The static pushover curve and the modal capacity curve are given in Fig. 8. The displacement demand of the building is found from Figs. 8(a), (b) as S_{de1}=0.134 m. Accordingly, the top displacement demand is found as given below.

$$S_{d1} = CR_1 \times S_{de1} = 1 \times 0.134 = 0.134\ m \tag{3}$$

$$u_{N1} = \Phi_{N1} \times \Gamma_{x1} \times d_1 = 0.076 \times 17.6644 \times 0.134 = 0.180\ m \tag{4}$$

The plastic hinges and shear forces which occurred in the 5th and last step of the pushover analysis are given in Figs. 9 (a), (b), (c), (d), (e), (f). Fig. 9(a) and Fig. 9(b) demonstrate the status

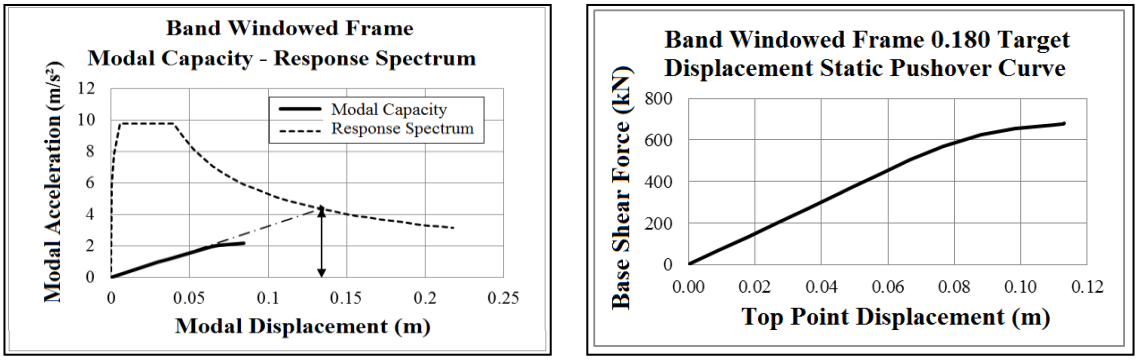

(a) (b)

Fig. 8 (a) Band-windowed frame superposed on the modal capacity and response spectrum (b) Band-windowed frame system target displacement pushover curve

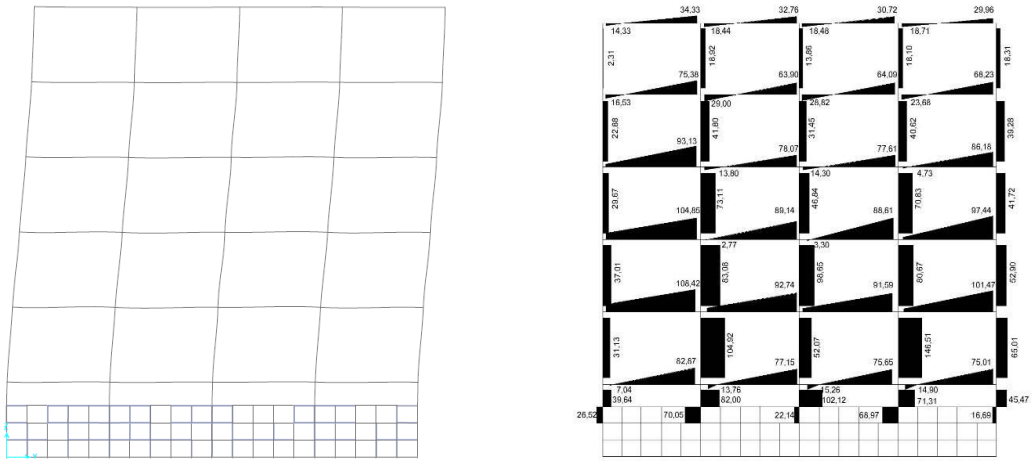

(a) (b)

Fig. 9 (a) Band-windowed frame system pushover analysis 5th step: plastic hinges, (b) Band-windowed frame system pushover analysis 5th step: shear forces, (c) Band window frame system pushover analysis 8th step: plastic hinges, (d) Band window frame system pushover analysis 8th step: shear forces, (e) Band-windowed frame system pushover analysis last step: plastic hinges, (f) Band-windowed frame system pushover analysis last step: shear forces

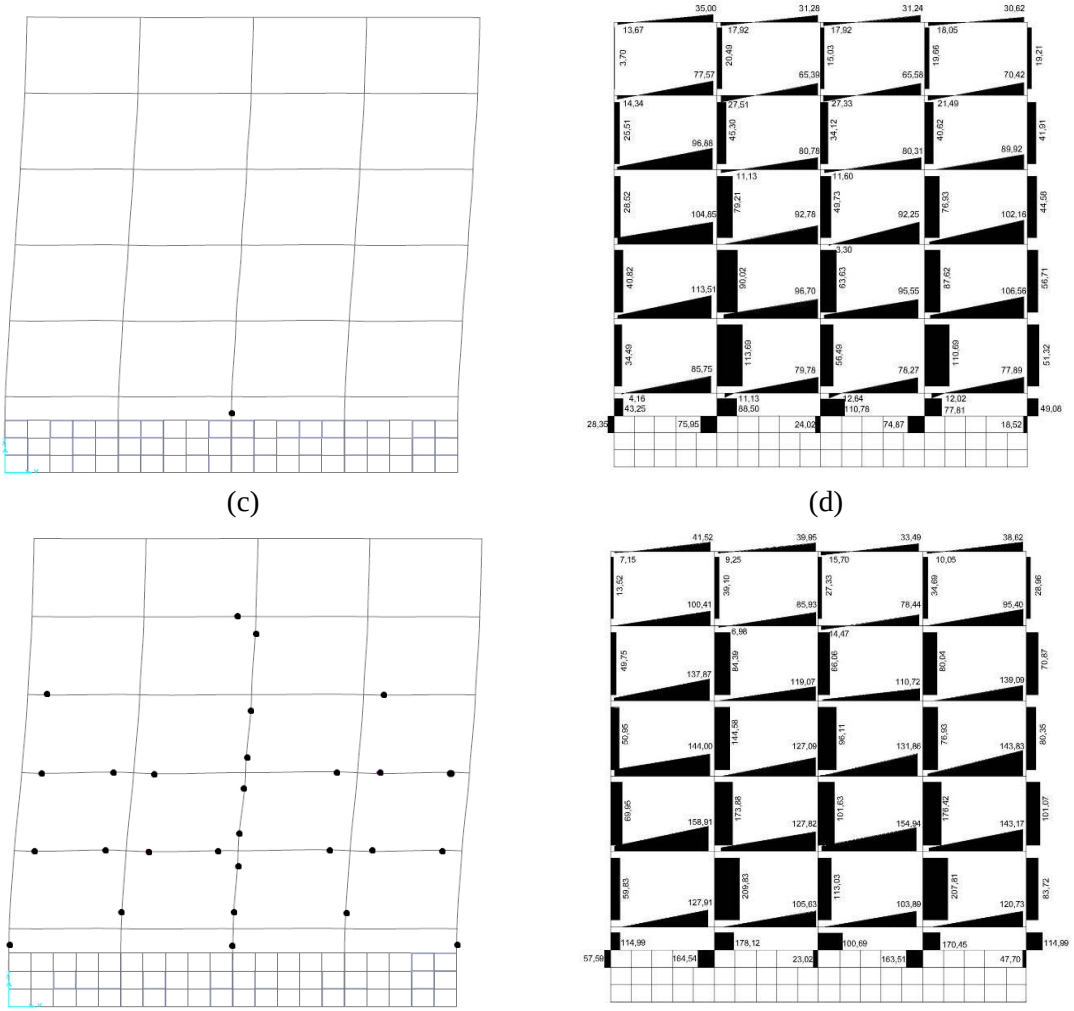

(c) (d)

(e) (f)

Fig. 9 Continued

before adding shear hinges to the columns of the band windows. As can be seen on column S103 there is a shear force with value 110.78 kN. Fig. 9(c) and Fig. 9(d) show the shear force and state of the hinges after installation of the shear hinges (8th step). As can be seen, the first hinge of the bare frame is caused by bending and in the case of the band window system, non-ductile damage occurs. Figs. 9(e) and 9(f) show the hinge status and shear force values in the last step before the system becomes unstable.

According to the results, it can be seen that displacement capacity of the bare frame is higher than the displacement demand of design earthquake and plane frame exhibits a ductile behavior. However, the building with short columns collapses before the target displacement and it exhibits a lower ductility compared to the bare frame.

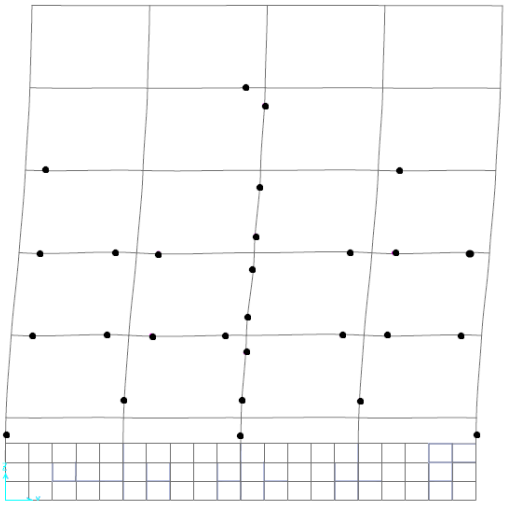

Fig. 10 Simulated ground motion records

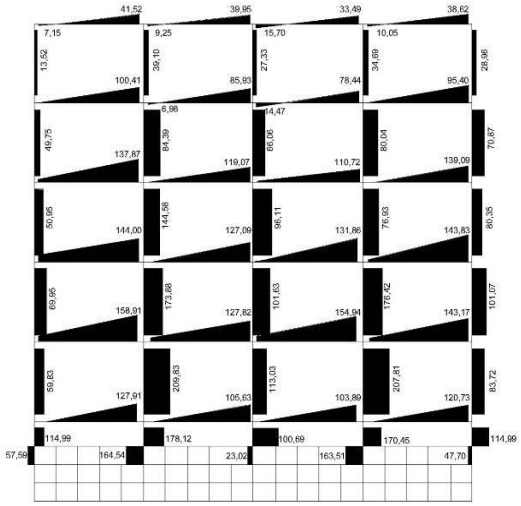

Fig. 11 Implementation of simulated ground movement records to the TSC'2007 Z2 Spectrum

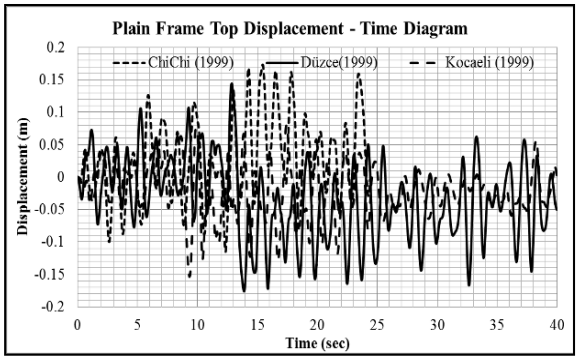

Fig. 12 Top displacement time history for the plain frame

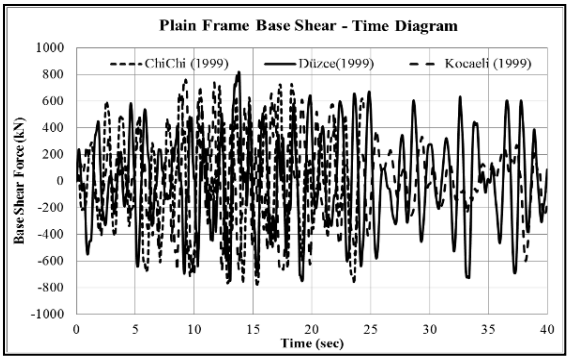

Fig. 13 Base shear time history for the plain frame

3. Nonlinear time history analysis

The considered systems were also subjected to nonlinear time history analyses. In order to be able to conduct an analysis in the time domain, the ground motion records of the Duzce (1999), Kocaeli (1999) and Chi-Chi (1999) Earthquakes are used to obtain the artificial ground motion and are then converted to the Z2 spectrum given in the TSC 2007. Fig. 10 shows simulated records according to this conversion and the converted records into the spectral acceleration - period. The Z2 spectrum is depicted in Fig. 11.

As results of the time history analyses, the top displacement value of the bare frame (Δ) for the Chi Chi (1999) Earthquake is 17.3 cm, for the Duzce (1999) Earthquake 14.4 cm and for the Kocaeli (1999) Earthquake 7.98 cm. Top displacement versus time is given in Fig. 12. The maximum base shear (V_t) is found as 822.23 kN for the Duzce (1999) Earthquake, while it is

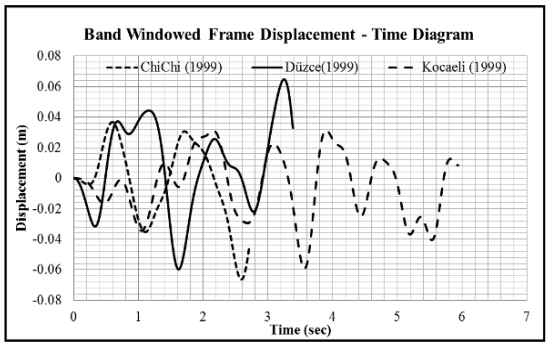

Fig. 14 Band-windowed top displacement versus time

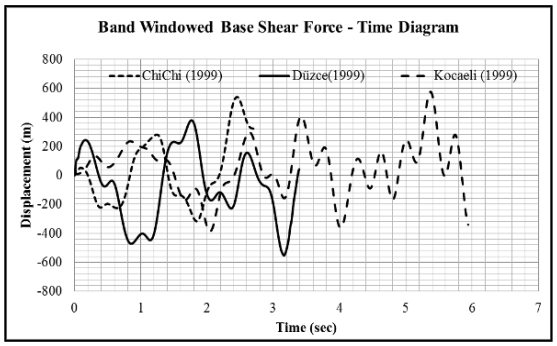

Fig. 15 Band-windowed base shear versus time

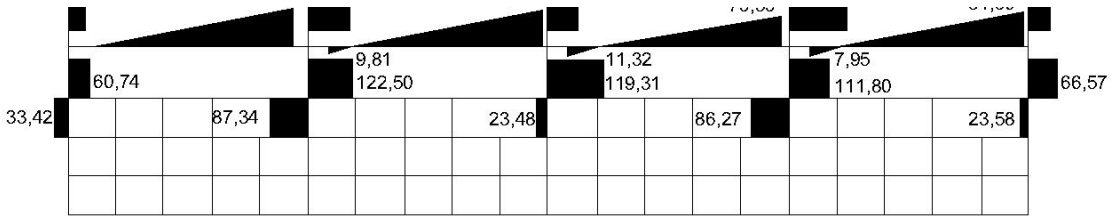

Fig. 16 Base shear occurring in the band-windowed frame.

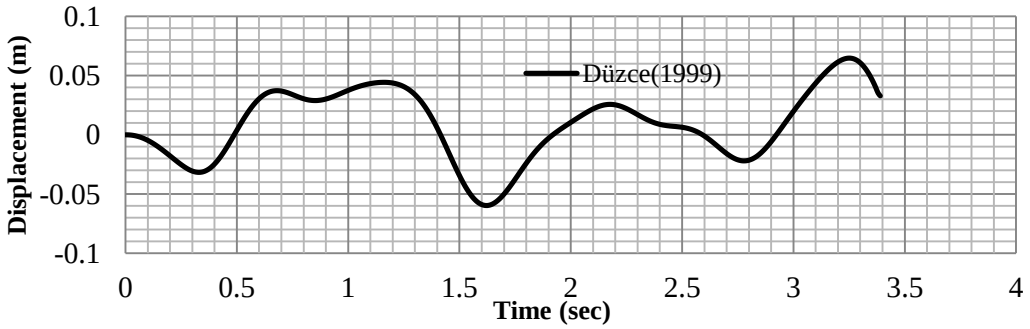

Fig. 17 Band-windowed frame: change of top displacement versus time obtained by using the Duzce (1999) Earthquake Records

730.24 kN for the Chi Chi (1999) Earthquake and 763.02 kN for the Kocaeli (1999) Earthquake. The base shear time history for bare frame is given in Fig. 13.

Evaluating the results of the static pushover and the time history analyses for the frame, it can be seen that the results are compatible. The effect of the basement curtain wall on the structural behavior of the short columns constructed at low level by the band windows' application is also examined. As a result of the time history analyses for the band window frame system, the top displacement value (Δ) for the Chi Chi (1999) Earthquake is 3.6 cm, for the Duzce (1999) Earthquake 6.47 cm and for the Kocaeli (1999) Earthquake 3.15 cm. The maximum base shear (V_t) is found as 540.7 kN for the Chi Chi (1999) Earthquake, 379.28 kN for the Duzce (1999) Earthquake and 575.91 kN for the Kocaeli (1999) Earthquake. The base top displacement time

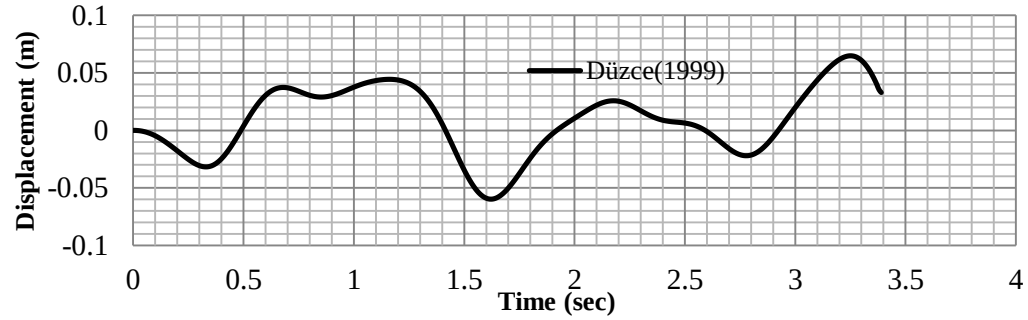

Fig. 17 Band-windowed frame: change of top displacement versus time obtained by using the Duzce (1999) Earthquake Records

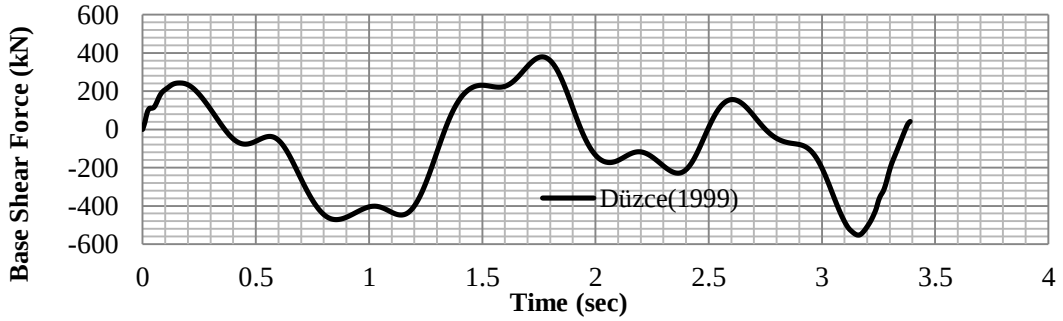

Fig. 18 Band-windowed frame: change of base shear versus time obtained by using the Duzce (1999) Earthquake Records

history and the base shear time history for the band-windowed frame is given in Figs. 14 and 15.

The shear forces that occurred on the short colums at t=3.39 s are given in Fig. 16.

As can be seen from Fig. 16, the shear force on the S103 column with a value of 119.31 kN is greater than the shear capacity of the column. As in the results of the pushover analysis, shear failure can also be seen in this column. In order to consider this situation, sliding hinges are assigned to the columns in order to determine the actual shear capacity. Thus, a real behavior model can be obtained. In the model with shear hinge definitions on the short columns of the band window application, the top displacement and base shear changes versus time results, (obtained from the time domain analysis of the Duzce (1999) Earthquake records) are given in Fig. 17 and Fig. 18.

4. Performance of FRP retrofitted short columns

In this study, performance improvement of columns is considered by increasing the shear capacity of the columns with fibrous polymer (LP) as given in Annex 7E of the TSC' 2007. The shear strength of LP-wrapped columns and beams is calculated with the following equation.

$$V_r = V_c + V_s + V_f \leq V_{\max} \tag{5}$$

Table 7 Technical specifications of carbon fiber polymer fabric with very high module

Specification of CFRP	
Elasticity module (N/mm^2), E_f	640000
Tensile strength (N/mm^2), f_u	2650
Design section thickness (mm), t_f	0.19
Breaking strain, ε_{fu}	0.004
Width (mm), b	300

Table 8 FRP- retrofitted columns' shear capacity

Shear capacity of columns after wrapping with LP							
Column no.	*bx* (cm)	*by* (cm)	V_{cr} (kN)	V_s (kN)	V_f (kN)	V_r (kN)	$V_{\max}$ (kN)
S101	40	30	159.64	54.55	179.968	362.24	351.12
S102	60	30	370.16	84.04	277.248	567.42	526.68
S103	30	60	87.67	39.81	131.328	241.27	526.68

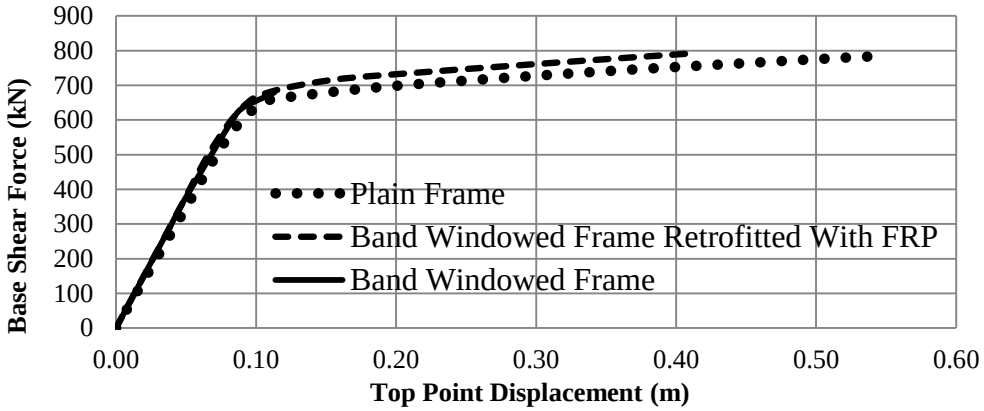

Fig. 19 Static pushover curve for "only frame", carbon-fibered short columns and sliding-hinged short column status

The contribution V_f of the LP wrapping to the shearing force is given with the following equation where it is wrapped in strips.

$$V_f = \frac{2 n_f t_f w_f E_f \varepsilon_f d}{s_f} \tag{6}$$

In the equation, n_f gives the number of LP coatings on one surface, t_f gives the effective thickness of LP for one coat, w_f gives the LP width, E_f stands for the LP elasticity module, ε_f gives the LP effective unit lengthening limit, d is the effective depth of the element and s_f is the space between the LP strips from axis to axis. In the case of applied continuous wrapping, it will be considered that w_f=s_f. The effective unit lengthening value is given below.

$$\varepsilon_f \leq 0.004 \tag{7}$$

$$\varepsilon_f \leq 0.50\varepsilon_{fu} \tag{8}$$

Technical specifications of the wrapping material, LP, are given in Table 7.

The effective unit lengthening value of FRP is ε_f=0.5×0.004=0.002. At the same time, the shear capacity of the columns never exceeds V_{max}=0.22×f_{cm}×b×d.

Table 8 was calculated by using Eqs. (5)-(6) which was given at the beginning of this section. The following table shows the shear capacity of the columns with the contribution of LP.

As can be seen from the results, the system can satisfy the displacement demand with a ductile damage distribution according to comparison of pushover results given in Fig. 19 and Fig. 20.

No shear hinge occurred at the ground floor columns of retrofitted building. The shear capacity and ductility of columns can be increased by using FRP and the short column problem can be avoided using FRP in a special rate (V_r<V_{cr}). The hinge status and shear force values in the last step before the system becomes unstable are given in Fig. 21 and Fig. 22.

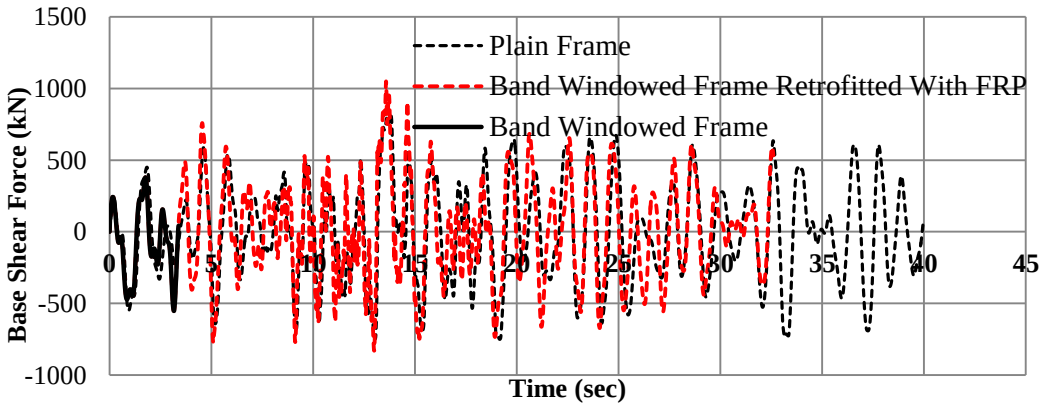

Fig. 20 Base shear change versus time, obtained as a result of a time domain analysis of "bare frame", carbon-fibered short columns and sliding-hinged short column status

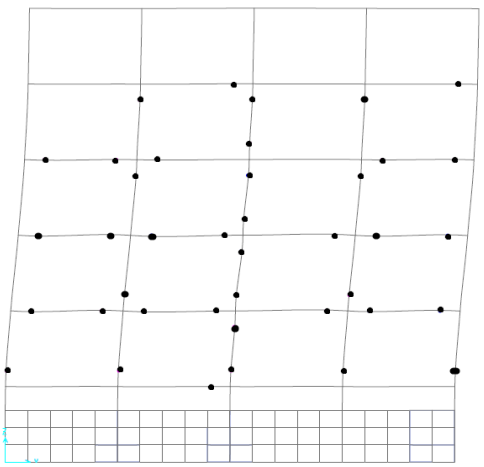

Fig. 21 FRP- retrofitted pushover analysis view

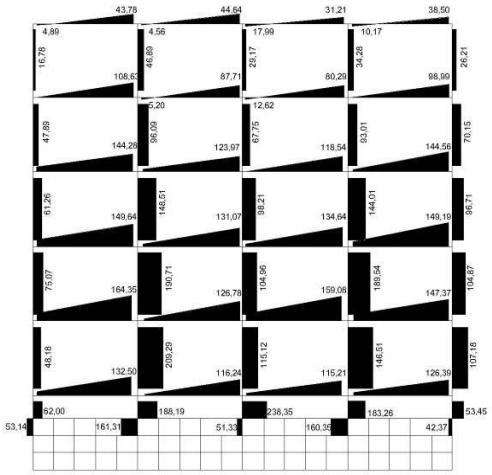

Fig. 22 FRP- retrofitted pushover analysis shear forces

5. Conclusions

Based on the results of a limited number of analyses for investigating band window effect on RC buildings by using previous earthquake data, the following conclusions can be listed,

• Due to seismic shaking, additional shear forces developed at joints. Especially, shear forces developed in short columns during earthquakes (119.31 kN) are much higher than the predicted design values (110.78 kN). In such cases, the elements are subjected to cracking and fails due to the shear force according to time history analysis.

• It can be easily seen from the analysis of the bare frame model that the required top displacement (0.54m) is much more than the earthquake displacement demand (0.153m). However, displacement demands (0.134m) are not satisfied in band-windowed framed structures (0.120m)

• On the other hand, expected earthquake resistant performance is achieved in the frames which consist of short columns retrofitted with FRP. It has been shown that brittle failure occurs with a lack of shear capacity. Moreover, the analysis results indicate that FRP retrofitting of short columns around band windows successfully increased the shear force carrying capacity of the short columns.

References

Chaallal, O., Shahawy, M. and Hassan, M. (2003), "Performance of axially loaded short rectangular columns strengthened with carbon fiber-reinforced polymer wrapping", *J. Compos. Constr*., ASCE, **7**(3), 200-208.

Chen, J.F. (2002), "Load-bearing capacity of masonry arch bridges retrofitted with fibre reinforced polymer composites", *Adv. Struct. Eng*., **5**(1), 37-44.

Colomb, F., Tobbi, H., Ferrier, E. and Hamelin, P. (2008), "Seismic retrofit of reinforced concrete short columns by CFRP materials", *Compos. Struct.*, **82**(4), 475-487.

Galal, K., Arafa, A. and Ghobarah, A. (2005) "Retrofit of RC square short columns", *Eng. Struct.*, **27**(5), 801-813.

Girgin, K. (1996), "A method of load increments for determining the second-order limit load and collapse safety of RC framed structures", Ph. D. Thesis, Dissertation, İstanbul Technical University, İstanbul.

Guevara, L.T. and Garcia, L.E. (2005), "The captive and short column effects", *Earthq. Spectra*, **21**(1), 141-160.

Hadi, M. N. S. (2006), "Comparative study of eccentrically loaded FRP wrapped columns", *J. Compos. Struct.*, **74**(2), 127-135.

Haskett, M., Mohamed Ali, M.D., Oehlers, J. and Wu, C. (2009), "Influence of bond on the hinge rotation of FRP plated beams", *Adv. Struct. Eng.*, **12**(6), 833-843.

Ilki, A., Peker, O., Karamuk, E., Demir, C. and Kumbasar, N. (2008), "FRP retrofit of low and medium strength circular and rectangular reinforced concrete columns", *J. Mater. Civil Eng*., ASCE, **20**(2), 169-188.

Ilki, A., Demir, C., Bedirhanoglu, I. and Kumbasar, N. (2009), "Seismic retrofit of brittle and low strength RC columns using fiber reinforced polymer and cementitious composites", *Adv. Struct. Eng.*, **12**(3), 325-347.

Koçak, A. (2013), "The effect of short columns on the performance of existing buildings", *Struct. Eng. Mech*., **46**(4), 505-518.

Kusumawardaningsiha, Y. and Hadi, M.N.S. (2010), "Comparative behaviour of hollow columns confined with FRP composites", *Compos. Struct.*, **93**(1), 198-205.

Paulay, T. (1991), "Seismic design strategies for ductile reinforced concrete structural wall", *Proceedings of International Conference on Buildings with Load Bearing Concrete Walls in Seismic Zones*, Paris, France.
Promis, G., Ferrier, E. and Hamelin, P. (2009) "Effect of external FRP retrofitting on reinforced concrete short columns for seismic strengthening." *Compos. Struct.*, **88**(3), 367-379.
Toutanji, H., Zhao, L. and Zhang, Y. (2006), "Flexural behaviour of reinforced concrete beams externally strengthened with CFRP sheets bonded with an inorganic matrix", *Eng. Struct.*, **28**(4), 557-566.
Turkish Earthquake Resistant Design Code (2007), TSC, Specifications for buildings to be built in disaster areas, Ankara.
Wang, Y. and Hsua, K. (2008), "Design of FRP-wrapped reinforced concrete columns for enhancing axial load carrying capacity", *Compos. Struct.*, **82**(1), 132-139.
Xiao, Y. (2004) ,"Applications of FRP Composites in Concrete Columns", *Adv. Struct. Eng.*, **7**(4), 335-343.
XTRACT, (2001), Cross Sectional Analysis of Components, Imbsen Software System, Sacramento.
Yoshimura, K., Kikuchi, K., Kuroki, M., Ozawa, K., Masuda, Y., Okino, M., Koja, T. and Tanaka, Y. (2000), "Experimental study on seismic behavior of R/C short columns retrofitted by carbon fiber sheets", *Composite and hybrid structures: Proceedings of the sixth ASCCS International Conference on Steel-Concrete Composite Structures*, 927-935.

CC